Seeded Crystal Growth onto Enamel Mineral and Synthetic Hydroxyapatite in Dilute Supersaturated Solutions Containing Low Concentrations of Fluoride

Chan Young Lee and Takaaki AOBA[1)]
Yonsei University, Depertment of Conseivative
and
[1)] *The Nippon Dental University, Department of Pathology, Tokyo Japan*

Abstract

The present study was undertaken to investigate the crystal growth onto enamel mineral and synthetic hydroxyapatite seeds in media resembling the enamel fluid composition. Effects of fluoride at low concentrations on the precipitation were also examined in a bench-top crystal growth model adopting a miniaturized reaction column. X-ray diffraction and Fourier transform infrared spectroscopy(FTIR), as well as chemical analyses, were employed for characterization of both seed materials before and after experimentation. Remarkable findings were that (1) both biological and synthetic seeds at the same total surface areas yielded rather similar precipitation rates at all levels of fluoride concentration in solution and (2) the precipitation rate was accelerated in a manner depending on fluoride concentrations in media. FTIR differential analysis disclosed that the precipitating phase was characterized as poorly crystallized apatite, which incorporated subtle carbonate. Most of the fluoride ions in soution were readily incorporated into crystals. The overall results support the view that the seeded crystal growth model is of value to gain insight into the mechanism of enamel crystal growth under fluoride regimens.

Key words : Enamel-Hydroxyapatite-Fluoride-Crystal Growth

Introduction

In the last decades, much attention has been focused on the regulatory mechanism of enamel mineralization during amelogenesis, since the enamel formation is a unique model in elucidating how bioapatite crystals grow to remarkable lengths and in a highly organized ultrastructure. A current consensus is that after the initial precipitation of octacalcium phosphate(OCP)-like precursor appearing as thin ribbons, the increase of mineralization is most adequately described by the growth of enamel crystals, not by increasing the number of crys-

tallites(Brown et al., 1987 : Cuisinier et al., 1990 : Iijima et al., 1992 : Miake et al., 1993). Crystal growth studies using various benchtop models have enhanced our understanding of the process and mechanism involved in enamel crystal growth. In those studies, synthetic hydroxyapatite crystals or other calcium phosphates were usually used as seeds to stimulate the process of enamel crystal growth. However, it still remains to be learned about whether possible differences in the composition, structure and properties between biological and synthetic products may provide distinct effects on the crystal growth kinetics and the nature of precipitating mineral phase(s). In particular, it is of extreme importance to elucidate wheter vestiges of organic matter on enamel crystals might affect the precipitation reaction onto enamel crystals. Another issue to be considered is effects of fluoride on the developmental enamel mineralization. Until now, it was demonstrated that fluoride ions are a unique regulator in biomineralization, which can accelerate the hydrolysis of acidic precursors(Tung et al., 1992 : Mura-Galelli et al., 1992) and the precipitation kinetics of apatite crystals(Vareghese and Moreno, 1981), giving rise to an increase in the stability of enamel mineral(Moreno et al. 1977).

On the basis of the foregoing consideration, the present study was aimed specifically to examine the differences or similarities of precipitation kinetics induced by enamel mineral and synthetic HA seeds and to assess fluoride effects on the precipitation taking place in those systems. To this end, we utilized a crystal growth model adopting a miniaturized reaction column, in which seed crystals were placed. This model was designed to simulate the mineralization process taking place in a narrow region adjacent to the secretory ameloblast, where the preformed enamel crystals (seeded apatite crystals *in vitro*) are exposed to a fluid flow at controlled rates to supply predetermined concentrations of lattice ions.

Materials and Methods

Experimental set-up for precipitation of calcium phosphates in in vitro model.

The general procedure used was the same as that previously described (Mura-Galelli et al., 1992). Two types of seed materials were used : (a) mature enamel mineral (EN) obtained from unerupted pig permanent incisors and (b) sythetic hydroxyapatite (HA). The preparation of pig enamel sample was as reported previously (Aoba and Moreno, 1990). This biological sample contained traces (less than 5 wt%) of organic matter. Synthetic crystal sample was prepared in aqueous system at neutral pH and 80℃ (Shimoda *et al.* 1990). EN crystals exhibited large platy morphology, while the synthetic crystals were composed of large, rod-like crystals, having elongated hexagonal cross-sections (data not included). The specific surface areas of EN and HA, determined by N_2 adsorption, were 9.8 and 24.5 m^2/g, respectively. Possible effects of seed materials of different specific surface areas were compared in the following crystal growth experiments conducted at the same total surface areas, or applying different masses.

Fig. 1 illustrates schematically the experimental set-up, which comprised vessel A containing the original experimental solution, a peristaltic pump to deliver a supersaturated solution at a constant rate, a reaction chamber made of a plastic column (0.5㎖ in volume), and vessle B to collect the experimental solution after it was passed through the column. A slurry of seed crystals was introduced through the top orifice into the column. As shown in the insert of Fig. 1 on an expanded

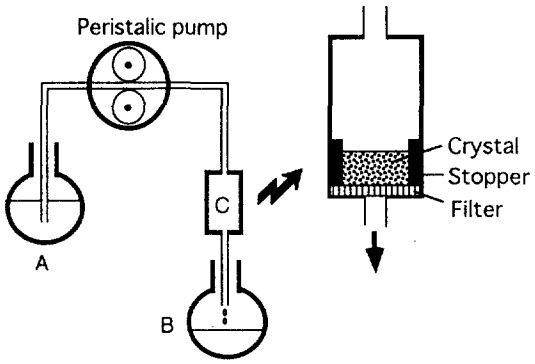

Fig. 1. Schematic illustration of experimental set-up seed crystals were placed in a minicolumn (C). Experimental solution, reserved in a large volume in vessel A, was delivered into the column at a constant rate with the aid of a peristaltic pump. The solution passed through the column was collected in vessed B. Insert : solid material was sedimented on a filter paper hold at the bottom end of the column with a plastic stopper.

scale, the crystals were allowed to sediment on a filter membrane (Whatman, Hillsboro, Orgeon) which was held with a plastic gasket placed at the bottom end of the column. During the experimental period, the column was kept in a vertical position by a clamp attached to a stand. In this fashion, the sedimented seed crystals were exposed continuously to a flow of the supersaturated solution, which was fed through the top orifice of the column at a constant rate with the peristaltic pump.

Experimental solutions were prepared from stock solutions of $CaCl_2$, KH_2PO_4, and Tris, In order to resemble the composition found in the secretory enamel fluid (Aoba and Moreno, 1987), the nominal soluion composition was 1mM Ca, 3mM of the total P, and 100mM Tris as background electrolyte. The pH values of the solutions were adjusted at 7.2 ± 0.2 with addition of minute volumes of dilute NaOH. The resulting solution was supersaturated with respect to both HA and OCP but was undersaturated with respect to dicalcium phosphate dihydrate. Our previous studies using the same crystal growth model evidenced that

Table 1. Chemical compsition of the original seed materials and solid samples recovered after crystal growth experiments

Sample	Ca wt%	P wt%	Mg wt%	Na wt%	HPO_4 %P	Ca/P
Enamel						
original	37.4	18.6	0.19	0.88	4.9	1.56
0.0ppm	38.3	18.4	0.16	0.64	7.2	1.61
0.1ppm	37.2	18.2	0.16	0.60	7.4	1.58
1.0ppm	37.5	18.4	0.13	0.47	9.2	1.58
Synthetic HA						
original	37.4	18.6	0.01	0.14	14.4	1.56
0.0ppm	37.7	19.2	0.02	0.13	13.3	1.52
0.1ppm	38.4	19.1	0.02	0.15	14.9	1.56
1.0ppm	38.0	19.1	0.02	0.06	17.8	1.54

there exist threshold fluoride concentrations : below 0.1ppm, the formation of OCP precursor having thin ribbon morphology is favorable but its hydrolysis is feasible, while, beyond 0.4ppm F, the formation of OCP is inhibited and the precipitation and growth of apatitic crystals becomes mostly favorable (Mura-Galelli et al., 1992). Taking into account those data, we tested here two fluoride concentrations, 0.1 and 1.0ppm, as well as 0ppm by no addition of fluoride.

In all systems, the precipitation reaction was conducted at room temperature (25 ± 2℃) under atmospheric pressure. Feeding rates of the solution were adjusted in the range of 2 to 3mℓ/h. The precipitation experiment was continued for 24h unless specified otherwise. At the end of all experiments, a total volume of the experimental solution exposed to the seed crystals was determined by weighing the solution collected in the vessel B. Both inlet (reserved in vessel A) and outlet (collected in vessel B) solutions were used for determination of concentrations of Ca, P and F, and values of pH. The solid material was recovered as a pellet on the filter. After freezedried, the solid sample was pulverized (homogenized) into fine powder in an agate mortar, prior to examination by X-ray diffraction and Fourier tranform infrared spectroscopy (FTIR).

Chemical analysis

The Ca and P concentrations of the inlet and outlet solutions were determined by atomic absorption spectrophotometry (Perkin Elmer model 3030) and colorimetry (Vogel, 1961), respectively. The pH values and the fluoride concentrations of the corresponding solutions were determined with ion-selective electrodes. The amounts of Ca, P, and F consumed for precipitation of minerals during the experimental period were obtined according to equation $i=\sum\{[i]i-[i]o\}\times V$, where $[i]i$ and $[i]o$ correspond to the concentrations of ionic species, i, in the inlet and outlet solutions, respectively, and V is the total volume of the experimental solution delivered during the experimental period. In order to determine the total Ca, P, Mg and Na contents of solid samples, accurately weighted amounts of the powder sample were dissolved completely with minimum volumes of 3 mol/L $HClO_4$ and then diluted with deionized water to yield appropriate concentrations of the ionic species to be determined. The total Ca and Mg concentrations of the resulting solutions were determined by atomic absorption spectrophotometry ; the Na was determined with the same instrument in the emission mode. Acid phosphate in both enamel and synthetic smaples was determined according to the heat-induced pyrophosphate method (Shimoda et al., 1991). Samples were heated in air at 550℃) for 24h. The formed pyrophosphate was hydrolyzed with 1mol/L $HClO_4$ at 100℃ for 1h. Hydrolyzed and non-hydrolyzed samples were analyzed for phosphate colorimetrically The amount of acid phosphate was obtained from the difference in the phosphate analysis of the two smaples.

X-ray diffraction and Fourier transform infrared spectroscopy

The diffraction pattern of the pooled enamel samples was recorded using a D/Max X-ray powder diffractometer (Rigaku USA, MA) equipped with a rotating anode and a graphite monochrometer. The diffractometer had the following settings : X-ray target, copper Kα (wavelength 1.54Å) ; voltage and current, 50 kV and 100mA ; receiving slit, 0.1mm ; step of data collection, 0.02(2θ)/min.

For FTIR analysis, about 1㎎ of powder samples was dispersed in a finely ground KBr

matrix with the agate mortar and pestle. The diffuse-reflectance absorption spectrum of the powder mixture was obtained in a Perkin-Elmer 1600 FTIR over the range of 4500 to 450 cm^{-1} with 4cm^{-1} resolution. Sixty-four spectral scans were usually conducted on each sample. The subtraction of background absorbance from the experimental spectrum and the determination of peak maxima in the spectra were obtained using a software provided by Perkin-Elmer. The same subtraction procedure was conducted in order to gain information about the spectral feature of precipiated minerals.

Results and Discussion

Fig. 2 shows x-ray diffraction patterns of enamel and synthetic HA seeds used. The pattern of EN indicated the preferred orientation of enamel crystals, due to its platy morphology, which was marked by the strong(300) reflection. HA displayed a characteristic pattern of hydroxyapatite. Since solid samples used in the required crystal growth experiments were limited (see Table 2), X-ray diffraction patterns were not obtained from those samples. As shown below, the nature of solid samples recovered at the end of all experiments were examined by FTIR.

Table 1 shows the chemical composition of EN and HA seed materials, as well as typical results of chemical analyses for solid samples recovered after crystal growth experiments. All data shown in this Table are averages of triplicate determinations. The estimated errors for determination of Ca, tatal P, Mg, Na, F and HPO_4 were 4%, 1.5%, 4%, 6%, 5%, and 6% of the analyzed quantities, respectively. Notable findings were that (1) both EN and HA samples exhibited similar contents with respect to the total Ca and P (as a result, their Ca/P molar ratios), (2) the contents of

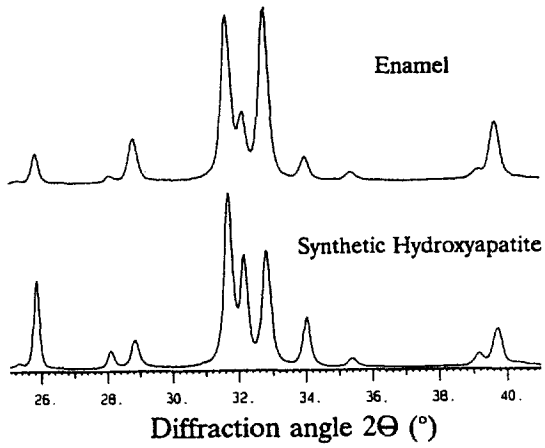

Fig. 2. X-ray diffraction patterns of enamel and synthetic hydroxyapatite used as seeds.

Table 2. Changes in solution composition after crystal growth upon seedings with either enamel or hydroxyapatite

Seed (mg)	[Ca] mM	[P] mM	pH	[F] ppm
Exp #1				
no seed	1.00	3.05	7.25	0.14
EN(8.3)	0.87	2.98	7.24	0.09
HA(3.0)	0.88	2.94	7.24	0.12
Exp #2				
no seed	1.01	3.04	7.25	0.11
EN(8.3)	0.78	2.90	7.23	0.04
HA(3.0)	0.79	2.89	7.23	0.05
Exp #3				
no seed	1.00	3.04	7.25	0.95
EN(8.3)	0.51	2.67	7.23	0.21
HA(3.0)	0.59	2.78	7.23	0.28

* The nominal concentrations of fluoride used in experiments
#1 through #3 were 0.0, 0.1, and 1.0 ppm, respectively.

Mg, Na, and HPO_4 were distinct between the biological and synthetic crystals, and (3) the composition of solid samples recovered after crystal growth experiments retained almost the same as that of the original seed crystals, except for an ascending trend of the HPO_4 found for EN.

A series of preliminary experiments showed that (1) no spontaneous precipitation (without addition of seed crystals) occurred within the experimental period in the experimental solution containing the highest concentration of fluoride and (2) subtle variations of the feeding rate did not cause a distinct difference in the amounts of the mineral precipitated and its nature. In Table 2 are shown typical results of changes in the ionic composition of the experimental solution after passing it through the column. In all systems, concentrations of the major lattice ions([Ca] and [P 10_4]) in the outlet solution decreased due to precipitation on the seed crystals. As assessed by those concentration changes, it was verified that the magnitude of crystal precipitation became more prominent as a function of fluoride concentration in experimental solution. The results also showed that most of the fluoride ions originally existing in solution were also incorporated into precipitating crystals, while the incorporation of (OH^-) as indicated by the dercrease of pH values was only marginal.

Fig. 3 shows changes in the rate of mineral precipitation upon seedings with either EN or HA. In this figure, the precipitation rate was expressed in terms of Ca or F ions(θg/h) consumed for precipitation per hour during the experimental period. In both systems using either EN or HA seeds, precipitation reaction accelerated steadily with increasing the fluoride concentration up to 1 ppm. The observation that apatite precipitation was accelerated in a manner depending on fluoride

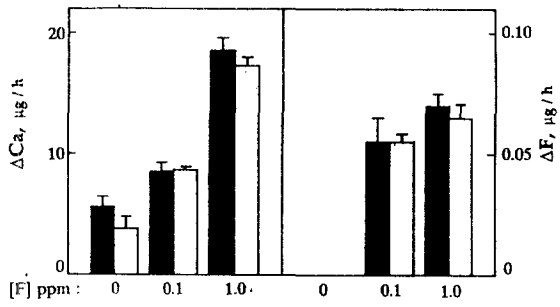

Fig. 3. Effects of fluoride in solution on precipitation of mineral onto seed crystals. The extent of precipitation reaction was expressed by the reduction in concentraions of Ca(left) and F (right), that is, the amounts of the lattice ions consumed for precipitation. The experimental data represented by solid and open columns were obtained in systems using enamel and hydroxyapatite seeds, respectively. All data are averages of analytical data obtained from the triplicate experiments.

concentrations in media, is in good agreement with the results previously obtained (Varughese and Moreno, 1981 ; Mura-Galelli et al., 1992). an underlying premise in the present work was that vestiges of enamel matrix proteins might affect the precipitation kinetics and the nature of precipitating solids. A result inconsistent with this line of thought was that, when weighing different masses to yield the same total surface area, both seeds from biological and synthetic sources yielded similar values of the precipitation rate at all levels of fluoride concentration in solution. It should be addressed that subtle differences existed between the two sets of kinetic data obtained using EN and HA seeds. As we previously discussed (Aoba and Moreno, 1984), the geometry of apatite crystals may affect their be-

havior as seeds for crystal growth. As supposed by x-ray diffraction patterns of EN and HA, it is a real possibility that they have distinct geometries. However, it is still astonishing that the biological and synthetic apatites that differ in their specific surface areas by a factor of two and half did exhibit rather similar behavior in crystal growth experiments.

Fig. 4 shows FTIR spectra of the original EN seed and solid samples recovered at the end of the experiments. The spectrum of the original seed crystals (Fig. 4A) was characterized by PO_4^{3-} bands at 564, 606, 962, 1034, 1098, 1102, and 1138 cm^{-1} and OH-band at 636 cm^{-1}. Three well-defined carbonate bands were also discernible at 1415, 1460, and 1545 cm^{-1}. As established in the literature (Elliott et al., 1985), the location of these maxima and the relative intensity of the bands indicate that type B carbonate (i.e., substitution into PO_4 sites) is dominant, while type A (i.e., substitution into OH sites) is also appreciable. Spectra in Fig. 4B and C were recorded from solid samples exposed to experimental solutions containing 0.1 and 1.0 ppm fluoride, respectively. A general feature of those spectra remained the same as that of the original seeds because the amounts of mineral precipitated were still marginal as compared to the total seed crystals added. However, the subtraction procedure between those experimental spectra allowed us to address the nature of precipitated mineral. A unique finding was that the obtained differential spectum was characterized by degeneration of the PO_4 bands in the wavenumber range of 1030 and 1100 cm^{-1}, a decrease in intensity of the OH-band, and the appearance of two broad bands at 870 and 1210 cm^{-1}. The last broad bands are assigned to protonated phosphate (Arend et al., 1987), consistent with the increase of the acid phosphate shown by chemical analysis. Collectively, the foregoing feature of FTIR spectra supports the precipitation of less crystallized apatitic salts, as compared with the original enamel crystals.

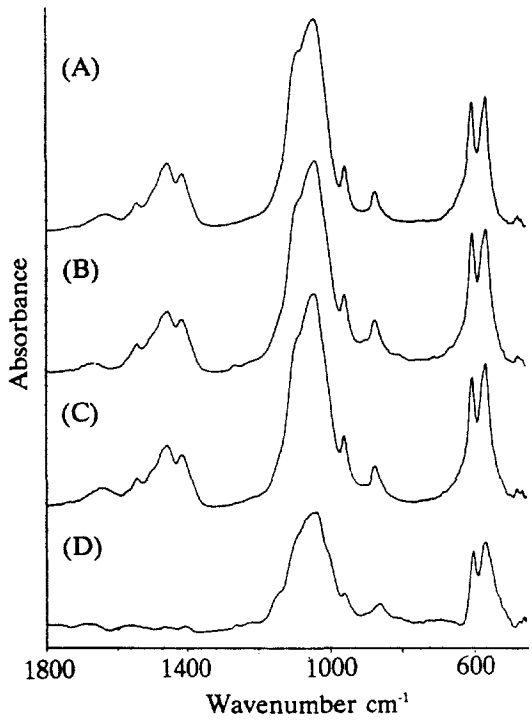

Fig. 4. FTIR spectra of pig enamel mineral. (A) Original seed crystals. (B and C) Solid samples recovered at the end of crystal growth experiments : Fluoride concentrations added to the experimental solution were (B) 0.1 ppm and (C) 1.0 ppm. (D) FTIR differential spectrum, which was obtained by subtracting spectrum A of the original seed crystals from spectrum C of the recovered solid sample.

Fig. 5 shows typical experimental and differential FTIR spectra of hydroxyapatite seeds. The spectrum of the original HA was distinct from that of EN, the absence of CO_3 bnads in particular (Fig. 5A). After crystal growth

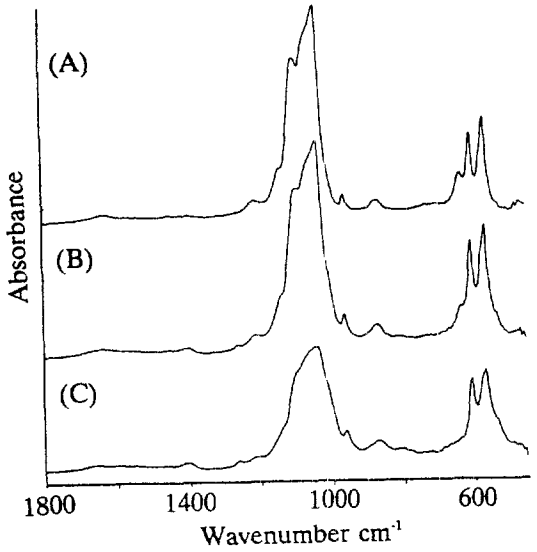

Fig. 5. FTIR spectra of synthetic hydroxyapatite. (A) Original seed crystals. (B) Solid sample recovered at the ent of crystal growth experiment with addition of 1.0 ppm fluoride. (C) FTIR differential spectrum between spectra A and B. Note the similar spectral feature to that shown in Fig. 4 C.

experiments, traces of the CO_3 bands became appreciable, in contrast to a decrease of OH band at 636 cm^{-1}, indicating the subtle incorporation of carbonate (mostly stemming from CO_2 in experimental solution) into precipitating apatite crystals. Notably, the spectral feature of the precipitated mineral (obtained by the subtraction procedure) resembled the corresponding spectrum shown in Fig. 4D.

In conclusion, the present results confirm that the *in vitro* precipition model, adopting a constant flow of the supersaturated solution through the miniaturized column containing seed crystals, is useful for assessment of the precipitation onto EN and HA seed crystals. It is of interest to note that precipitation reactions upon seedings, and the nature and properties of precipitated minerals, were not markedly affected by the source of seed materials, which were distinct with respect to the contents of minor lattice constituents, as well as the specific surface areas and morphology. The overall results indicate that the seeded crystal growth models are of value to gain insight into the mechanism of enamel crystal growth under fluoride regimens.

References

Aoba T, Moreno EC (1984) Preparation of Hydroxyapatite Crystals and Their Behavior as Seeds for Crystal Growth. J Dent Res 63 : 874−880.

Aoba T, Moreno EC. (1987) The enamel fluid in the early secretory stage of porcine amelogenesis. Chemical compostition and saturation with respect to enamel mineral. Calcif Tiss Int. 41 : 86−94.

Aoba T, Moreno EC. (1990). Changes in the nature and composition of enamel mineral during porcine amelogenesis. Calcif. Tissue Int 47 : 356−364.

Arend J., Christoffersen J., Christoffersen M. R., Eckert, H., Fowler, B.O., Heughebaert, J.C., Nancollas, G.H., Yesinowski, J.P. and Zawacki, S.J. (1987) A calcium hydroxyapatite precipitated from an aqueous solution. An international multimethod analysis. J Crystal Growth 84 : 515−532.

Brown WE, Eidelman N, Tomzaic BB. (1987). Octacalcium phosphate as a precursor in biomineral formation. Adv. Dent. Res. 1 : 306−313.

Cuisinier FJG, Steuer P, Frank RM, Voegel JC. (1990). High resolution electron microscopy of young apatite crystals in human fetal enamel. J Biol Buccale. 18 : 149−154.

ELLIOTT, J.C. ; HOLCOMB, D.W. YOUNG,

R.A. (1985) : Infrared Determination of the Degree of Substitution of Hydroxyl by Carbonate Ions in Human Dental Enamel, Calcif Tiss Int 37 : 372−375.

Iijima M, Tohda H, Moriwaki Y. (1992a). Growth and structure of lamellar mixed crystals of octacalcium phosphate and apatite in a model system of enamel formation. J. Crystal Growth. 116 : 319−326.

Miake Y, Shimoda S, Fukae M, Aoba T. (1993). Epitaxial overgrowth of apatite crystals on the thin-ribbon precursor at early stages of porcine enamel mineralization. Calcif. Tissue Int. 53 : 249−256.

Moreno EC, Kresak M, Zahradnik RT. (1977). Physicochemical aspects of fluoride-apatite systems releavant to the study of dental caries. Caries Res. 11 (Suppl. 1) : 142−171.

Mura-Galelli MJ, Narusawa H, Shimada T, Iijima M, Aoba T. (1992). Effect of fluoride on precipitation and hydrolysis of octacalcium phosphate in an experimental model simulating enamel mineralization during amelogenesis. Cells Materials. 2 : 221−230.

Shimoda S, Aoba T, Moreno EC. (1991). Changes in acid phosphate content in enamel mineral during porcine amelogenesis. J. Dent. Res. 70 : 1516−1523.

Shimoda S, Aoba T, Moreno EC, Miake Y. (1990). Effect of solution composition on morphological an structural features of carbonated calcium apatites. J. Dent. Res. 69 : 1731−1740.

Tung MS, Tomazic B, Brown WE. (1992). The effects of magnesium and fluoride on the hydrolysis of octacalcium phosphate. Archs Oral Biol. 37 : 585−591.

Varughese K, Moreno EC. (1981). Crystal growth of calcium apatites in dilute solutions containing fluoride. Calcif Tissue Int. 33 : 431−439.

Vogel AJ. (1961). Quantitative Inorganic Analysis, 3rd ed, New York. John Wiley & Sons : 810.